NASA TECHNICAL MEMORANDUM

NASA TM X-1748

NASA TM X-1748

CORRELATION OF GAS-SIDE HEAT TRANSFER FOR AXISYMMETRIC ROCKET ENGINE NOZZLES

by Uwe H. von Glahn

Lewis Research Center
Cleveland, Ohio

NATIONAL AERONAUTICS AND SPACE ADMINISTRATION • WASHINGTON, D. C. • FEBRUARY 1969

NASA TM X-1748

CORRELATION OF GAS-SIDE HEAT TRANSFER FOR AXISYMMETRIC ROCKET ENGINE NOZZLES

By Uwe H. von Glahn

Lewis Research Center
Cleveland, Ohio

NATIONAL AERONAUTICS AND SPACE ADMINISTRATION

For sale by the Clearinghouse for Federal Scientific and Technical Information
Springfield, Virginia 22151 – CFSTI price $3.00

ABSTRACT

Empirical correlating equations were developed to predict gas-side heat transfer for nozzles without a wall temperature step change near the nozzle entrance (such as regeneratively cooled rocket engines) over a wide range of conditions and configurations. The use of the reference enthalpy method for predicting fluid properties in these equations facilitated the correlation of heated air and rocket firing data.

CORRELATION OF GAS-SIDE HEAT TRANSFER FOR AXISYMMETRIC ROCKET ENGINE NOZZLES

by Uwe H. von Glahn

Lewis Research Center

SUMMARY

Experimental heat-transfer data for nozzles obtained from heated air and rocket firing tests were empirically correlated. The data include a range of nozzle contraction ratios from 2.83 to 19, contraction cone half-angles from 30° to 60° and nozzle diameters from 0.124 to 0.416 foot (0.0378 to 0.127 m). Because of the complexity of nozzle heat transfer, correlation required the use of several equations in order to accommodate the several heat-transfer regimes associated with nozzle heat transfer. The correlating equations are based on deviations of heat transfer from fully turbulent pipe flow values. The use of the reference enthalpy method for predicting fluid properties in these equations facilitated the correlation of heated air and rocket firing data. The correlation is limited to nozzles without a step change in wall temperature near the nozzle inlet (e.g., regeneratively cooled rocket engines).

INTRODUCTION

In order to preserve structural integrity, rocket nozzle walls must be cooled. The high heat flux levels associated with regeneratively cooled rocket nozzles, however, can cause the cooling capacity of the coolant fluid to become marginal. Accurate knowledge of the gas-side heat transfer is needed, therefore, in order to help determine the cooling load.

In the past, turbulent pipe flow heat-transfer correlations neglecting pressure gradient effects have been used to try to predict the gas-side heat transfer. Coefficients so calculated are greater than those obtained in tests with rocket-type nozzles. The lower experimental coefficients are attributed to the effect of flow acceleration on the velocity and thermal gradients in the boundary layer within the nozzles. A number of analyses have attempted to account for this effect (refs. 1 to 7, among others). These approaches,

however, have met with only limited success in correlating the growing mass of nozzle heat-transfer data.

In the present study, conducted at the NASA Lewis Research Center, empirical equations have been developed to predict heat transfer with flow through axisymmetric nozzles that have an initially turbulent or near-turbulent boundary layer at the nozzle entrance. Data correlation has been based on extended turbulent pipe-flow heat-transfer equations. The prime factors that appear to affect the local heat-transfer coefficients in a nozzle include nozzle geometry, area ratio, entrance region effects, and local fluid properties. The latter are based on reference enthalpy and static pressure for each nozzle station. The results of the present study are believed applicable, for engineering purposes, to current rocket nozzle sizes and various propellant combinations provided no step change in wall temperature occurs near the nozzle entrance and the nozzle entrance boundary-layer condition, mentioned previously, is met.

The unpublished heated air data cited herein were provided by Mr. Donald Boldman while the unpublished rocket firing data were provided by Mr. Ralph Schacht (H_2-O_2 rocket) and Mr. Fred Glaser (JP-GOX), all of the NASA Lewis Research Center.

BACKGROUND

Empirical correlations for heat transfer that do not directly consider boundary-layer concepts generally are expressed in simple geometric terms and fluid properties. As an example, conventional fully developed pipe-flow heat transfer can be obtained by the well-known Stanton form wherein:

$$St = \frac{Nu}{RePr} = \frac{KRe^{m} Pr^{n}}{RePr} \tag{1}$$

(All symbols are defined in the appendix.) While the choice of K, m, and n depends somewhat on the investigator and the manner in which data were obtained, the present work uses the following general equation (used also in ref. 5) as the basis for the correlation of nozzle heat-transfer data:

$$St = 0.026\ Re^{-0.2} Pr^{-0.7} \tag{2}$$

Experimental data (e.g., ref. 5) has shown that equation (2) does not represent heat transfer with accelerating flow through an axisymmetric nozzle. These latter data show that the deviation of nozzle heat transfer from that predicted by pipe-flow correlations depends on axial station in the nozzle, Reynolds number, nozzle geometry, and nozzle

entrance conditions. A brief discussion of the effects of these factors on nozzle heat transfer is contained in the following sections.

Nozzle heat transfer without step change in wall temperature near nozzle inlet. - Typical heat-transfer coefficients for a nozzle without a step change in wall temperature near the nozzle entrance (e.g., a regeneratively cooled rocket engine (ref. 5) or a cooled inlet-nozzle configuration (ref. 7)) are shown in figure 1 as a function of axial distance from the nozzle entrance. Immediately apparent from this figure is the fact that two distinct primary regimes exist in nozzle heat transfer as shown by curves A and B. Curve A

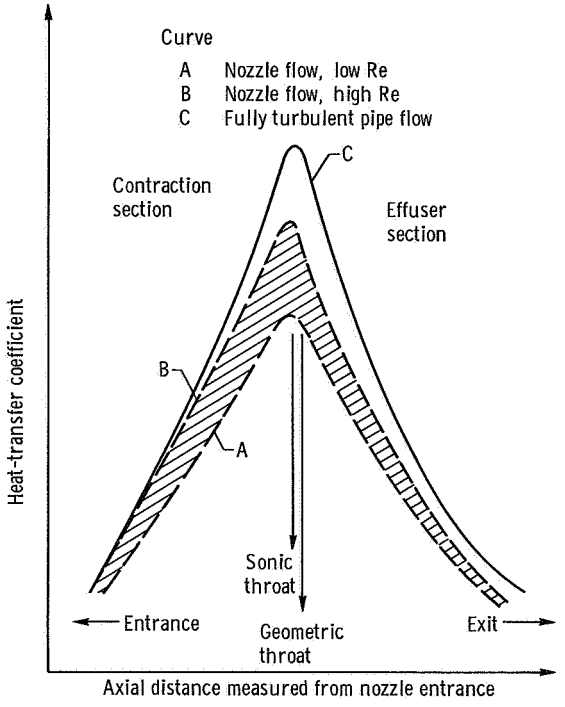

Figure 1. - Typical variation of nozzle heat-transfer coefficient with axial distance and comparison with fully turbulent pipe flow prediction.

represents nozzle heat-transfer data at relatively small Reynolds numbers (laminar-like magnitudes), whereas curve B represents data at large Reynolds numbers (turbulent-like magnitudes). Absolute values for the Reynolds numbers in each range are not given since they depend on nozzle geometry factors and fluid properties. The cross-hatched region between these curves represents transition heat-transfer values between low and high values of Reynolds number. Also shown in the figure is curve C, representing fully turbulent pipe-flow heat-transfer values. It should also be noted that the nozzle heat-transfer coefficients at small Reynolds numbers appear to deviate from pipe-flow predictions beginning at the nozzle entrance. At large Reynolds numbers a significant deviation

from pipe-flow values does not begin until well downstream of the nozzle entrance. Variations in local heat transfer caused by local flow separation or shock interactions (effuser section) are neglected in the representations of figure 1. A discussion of these phenomena is contained in reference 3. The effects of stream turbulence level upstream of the nozzle entrance on nozzle heat transfer were found to be generally small (refs. 4 and 7) and are also neglected.

The heat-transfer phenomena discussed previously will now be examined in closer detail in order to establish bases necessary for the correlation of available data.

The heat transfer near the throat region presents a critical cooling problem for the design of a rocket nozzle. The influence of Reynolds number on the deviation of nozzle heat transfer from fully turbulent pipe-flow values will be examined first in this region. Curves representing typical heat transfer obtained experimentally are plotted in figure 2 as a Stanton-Prandtl grouping φ (where $\varphi = \mathrm{StPr}^{0.7}$) against throat Reynolds number. Also shown is a curve representing fully turbulent pipe-flow heat transfer in terms of φ.

The curves representing the experimental data in figure 2 can be grouped into three primary heat-transfer regimes. The initial region, shown by line 1-2 occurs over a range of relatively low Reynolds numbers. In this region, heat-transfer reductions from pipe-flow values as much as 80 percent can be obtained. In fact, the nozzle heat-transfer values frequently approach those predicted from laminar pipe flow correlations.

At a particular throat Reynolds number (fig. 2, point 2), which depends on the specific nozzle configuration, the nozzle heat transfer undergoes a transition toward turbulent

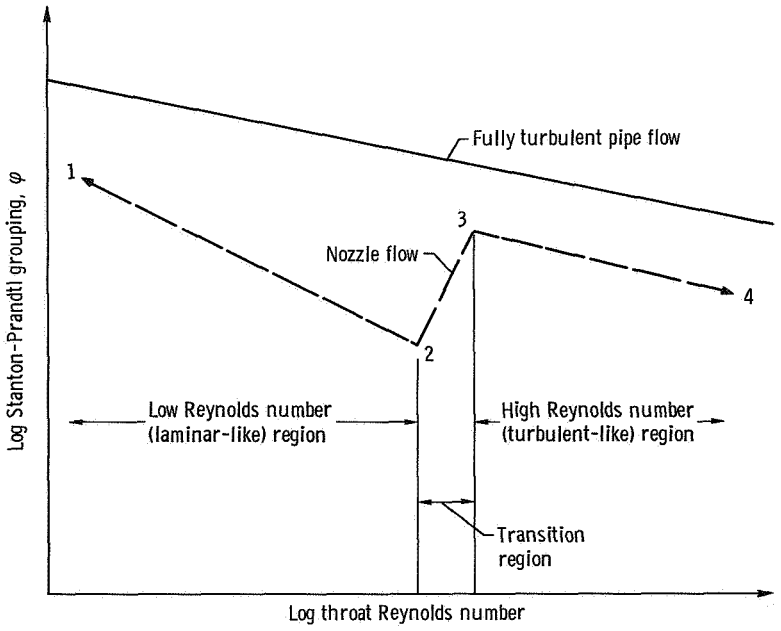

Figure 2. - Comparison of typical variation of nozzle heat transfer at throat station with fully turbulent pipe flow heat transfer.

flow heat transfer. In the transition region (fig. 2, curve 2-3) the difference in nozzle heat transfer from that predicted by pipe flow becomes less with increasing values of throat Reynolds number until a minimum difference is reached (fig. 2, point 3).

With further increases in the throat Reynolds number (fig. 2, curve 3-4) the difference in nozzle heat transfer from that predicted by pipe flow again increases but at a lower rate than that for region 1-2.

For other axial stations upstream of the throat, trends similar to those shown in figure 2 for the nozzle throat region are also observed. The heat-transfer reductions from pipe flow at local stations in a nozzle are generally less than those measured at the throat.

In the divergent section (effuser) of a nozzle, heat transfer can be quite complex. Factors such as combustion gas composition (equilibrium or frozen), shock interactions, and separated flow regions tend to affect heat transfer either locally or downstream. The present study considers only nozzles that are flowing full and in which the gas is in the equilibrium state.

When the effuser flows full, the heat-transfer values are lower than those predicted from pipe-flow equations. The reduction in nozzle heat transfer from that for pipe flow becomes less with increasing axial distance downstream of the nozzle throat. Examination of data from reference 6 (low subsonic flow throughout the nozzle) indicates that the recovery of the nozzle heat-transfer values to those for pipe flow occurs more rapidly for a constant cross-section pipe downstream of the throat (no divergence) than when an effuser is used (as in the other studies cited herein).

Nozzle heat transfer with step change in wall temperature near nozzle inlet. - Nuclear rocket nozzle designs frequently have the core exit located just upstream of the nozzles entrance. Such a nozzle generally can be expected to have a step change in wall temperature near the nozzle entrance. Introduction of a cooled mixing section between the core and nozzle would reduce or eliminate this temperature-step effect. For most chemical rocket nozzles the cooled combustion chamber can be considered as a cooled approach section. For a cooled nozzle with an uncooled approach section, a step change in temperature at or near the nozzle entrance causes higher heat-transfer coefficients than those for a nozzle with a cooled approach (refs. 6 to 8). Such increased coefficients can be explained as "entrance" or "starting" region effects involving the interaction of the boundary-layer velocity and temperature profiles. The higher values of heat transfer decrease with distance downstream of the start of the temperature step change as equilibrium between the velocity and temperature profiles is reestablished. When the influence of the temperature step change is large enough, even the throat heat transfer is greater for a nozzle with an uncooled approach section than that obtained with a cooled approach section. A typical example of this phenomena, taken from 2-dimensional nozzle data in reference 6 is shown in figure 3.

Heated-air data from reference 9 for a small nozzle with a short contraction section

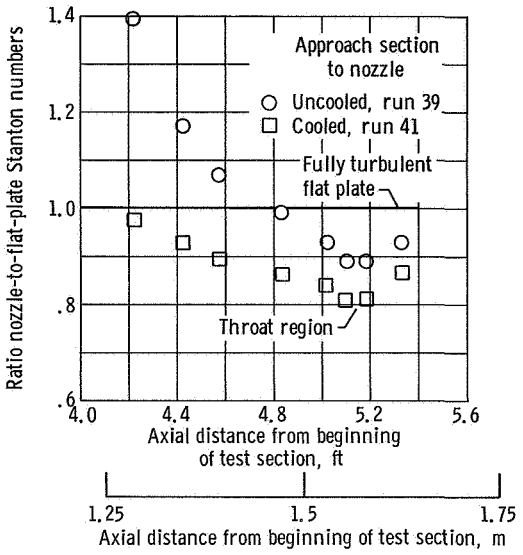

Figure 3. - Effect of step change in temperature near nozzle entrance on nozzle heat transfer. Cooled nozzle; data from reference 6.

(cone half-angle, 60^{o}) indicates that for some operating condition the heat transfer at the nozzle throat substantially exceeds values predicted from turbulent pipe flow (eq. (2)).

NOZZLE HEAT-TRANSFER CORRELATION

The proposed correlation treats nozzle heat transfer as a departure from fully turbulent pipe-flow heat transfer for cooled nozzles with a cooled approach section. This concept applies to both the low Reynolds number and high Reynolds number regions noted in figure 2. It also applies to the entire nozzle, whether convergent or divergent, provided that the previously mentioned criteria concerning the expansion process are satisfied. Thus the proposed correlation consists of a fully turbulent pipe-flow heat-transfer equation modified by suitable nozzle geometry parameters. The variables included in these parameters are summarized in figure 4 and table I.

In arriving at the proposed correlation equations, heat-transfer relations were developed first for the geometric throat station and then extended to accommodate heat transfer at local axial stations. Fluid properties used in the correlating equations were determined by the reference enthalpy method described in reference 5.

The following sections detail the correlating equations for the throat region, contraction section and finally the diverging section of a nozzle.

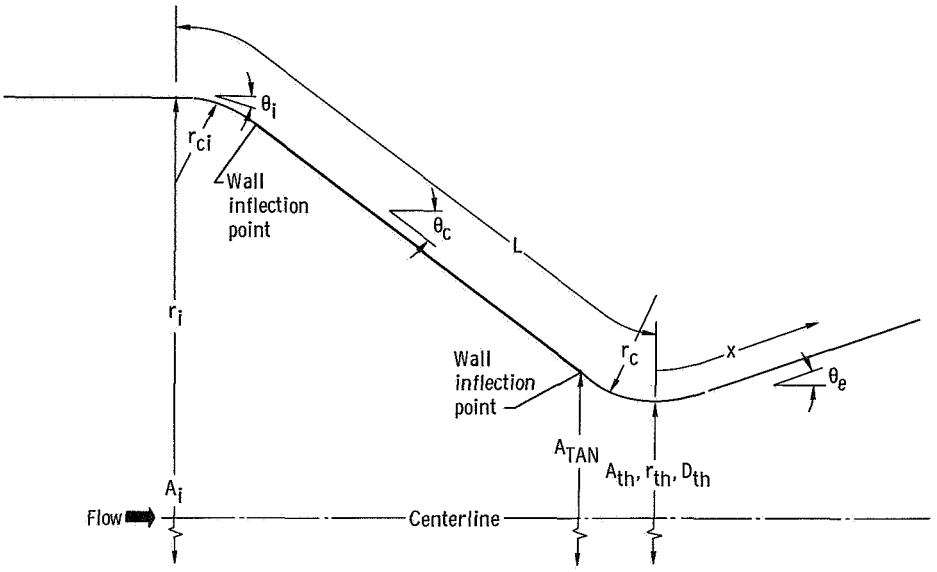

Figure 4. - Pertinent geometric variables used in data correlation. See appendix for symbol definitions.

Nozzle Throat

The departure of heat transfer at the nozzle throat from that for turbulent pipe flow is assumed to follow an empirical relation given by:

$$\varphi_{th} = \varphi_{pf}\left(\frac{C}{C + Re}\right)^{a} \tag{3}$$

where $\varphi_{pf} = (StPr^{0.7})_{pf} = 0.026\ Re^{-0.2}$, and Re is the local Reynolds number; in this case Re_{th}. The values of C and a are evaluated for the low or high Reynolds number regions (fig. 2) by the following equations.

Low Reynolds number region:

$$\varphi_{th,L} = \varphi_{pf}\left(\frac{C_L}{C_L + Re_{th}}\right)^{a_L} \tag{4}$$

where

$$C_L = \left(0.425 \frac{A_i}{A_{th}}\right)^{3.0} \tag{5}$$

and

$$a_L = 0.0875\left(\frac{A_i}{A_{th}} - 1\right)^{0.5}\left(\frac{\sqrt{\sin \theta_c}}{1 + \tan \theta_c}\right)^{0.5}\left[1 + \left(1 - \sin \theta_c\right)^5\right]\left(\frac{1}{1 + \frac{r_{ci}}{r_i}}\right)^{0.33} \tag{6}$$

TABLE I. - PERTINENT NOZZLE DIMENSIONS

Nozzle contraction ratio, A_i/A_{th}	Nominal throat diameter, D_{th}		Ratio of surface distance from nozzle inlet to throat to throat diameter, L/D_{th}	Cone half-angle in contraction section, θ_c, deg	Ratio of wall radius of curvature at throat to throat radius, r_c/r_{th}
	ft	m			
19.0	0.124	0.0378	3.50	30	2.0
4.29	↓	↓	2.0	30	↓
19.0			2.35	60	
4.29			1.7	60	
7.75	.15	.0457	2.16	30	
9.75	.133	.0406	1.79	45	.625
2.83	.220	.0674	1.24	30	2.0
4.64	.416	.127	1.67	30	1.0

Nozzle contraction ratio, A_i/A_{th}	Ratio of wall radius of curvature at inlet to nozzle inlet radius, r_{ci}/r_i	Ratio of area at tangency point to throat area, A_{TAN}/A_{th}	Reference
19.0	0	1.61	7 and unpublished NASA data
4.29	↓	1.61	7 and unpublished NASA data
19.0		4.0	7 and unpublished NASA data
4.20		4.0	Unpublished NASA data
7.75	.565	1.61	4
9.75	.32	1.41	3
2.83	1.0	1.70	Unpublished NASA data
4.64	2.13	1.96	5 and unpublished NASA data

High Reynolds number region:

$$\varphi_{th,T} = \varphi_{pf}\left(\frac{C_T}{C_T + Re_{th}}\right)^{a_T} \tag{7}$$

where

$$C_T = 400\left(\frac{A_i}{A_{th}}\right) \tag{8}$$

and

$$a_T = 0.1235\left(\frac{A_i}{A_{th}} - 1\right)^{0.5}\left(\frac{\sqrt{\sin\theta_c}}{1 + \tan\theta_c}\right)^{0.8}\left[1 + \left(1 - \sin\theta_c\right)^5\right]\left[\frac{\left(\frac{r_c}{r_{th}}\right)^{1.5}}{\left(\frac{r_c}{r_{th}}\right)^{2.5} + 0.575}\right] \tag{9}$$

Transition region:

In order to bridge between the low and high Reynolds number curves, a transition-region heat-transfer equation was developed. On the basis of data plots, a square-law Reynolds number criteria was assumed for this equation as follows:

$$\varphi_{th,Tran} = \left(\varphi_{th,T}\right)_{Re_{TT}}\left(\frac{Re_{th}}{Re_{TT}}\right)^{2.0} \tag{10}$$

where Re_{TT} is the throat Reynolds number at which transition from high Re to low Re heat transfer begins. The value of Re_{TT} is calculated from:

$$Re_{TT} = 1000\, f\left[\left(\frac{A_i}{A_{th}}\right), \left(\frac{r_c}{r_{th}}\right), (\theta_c), \left(\frac{L}{D_{th}}\right)\right] \tag{11}$$

where

$$f\left(\frac{A_i}{A_{th}}\right) = \left(\frac{A_i}{A_{th}} - 1\right)^{2.0}\left[1 + \left(\frac{7.65}{\frac{A_i}{A_{th}} - 1}\right)^{3.0}\right] \tag{12}$$

$$f\left(\frac{r_c}{r_{th}}\right) = \left(\frac{r_c}{r_{th}}\right)^{2.0}\left[1 + \frac{0.275}{\left(\frac{r_c}{r_{th}}\right)^{8.0}}\right] \tag{13}$$

$$f(\theta_c) = \left(1 - \frac{\sqrt{\sin\theta_c}}{1 + \tan\theta_c}\right)^{0.33} \tag{14}$$

and

$$f\left(\frac{L}{D_{th}}\right) = \left[\frac{\left(\frac{L}{D_{th}}\right)^{3.0}}{0.0935\left(\frac{L}{D_{th}}\right)^{4.67} + 0.4}\right] \tag{15}$$

Of these four functions, the $f(r_c/r_{th})$ is the least documented in the literature and therefore the most doubtful parameter in equation (11). The transition region terminates when $\varphi_{th,\,Tran}$ equals $\varphi_{th,\,L}$ at the same Re_{th} value. This value of Reynolds number $(Re)_{TL}$ can be established by trial and error calculations or, more simply by plotting equations (2) and (4) as a function of Re_{th} on log-log coordinates and drawing a straight line with a square law slope from Re_{TT} on the high Re curve to the intersection of this straight line with the low Re curve.

A comparison of experimental nozzle heat-transfer data at the throat station with values calculated by use of the preceding equations is shown in figure 5. The data are shown in terms of φ as a function of Re_{th}. The experimental data were obtained from references 3, 4, 5, and 7 as well as some unpublished NASA studies.

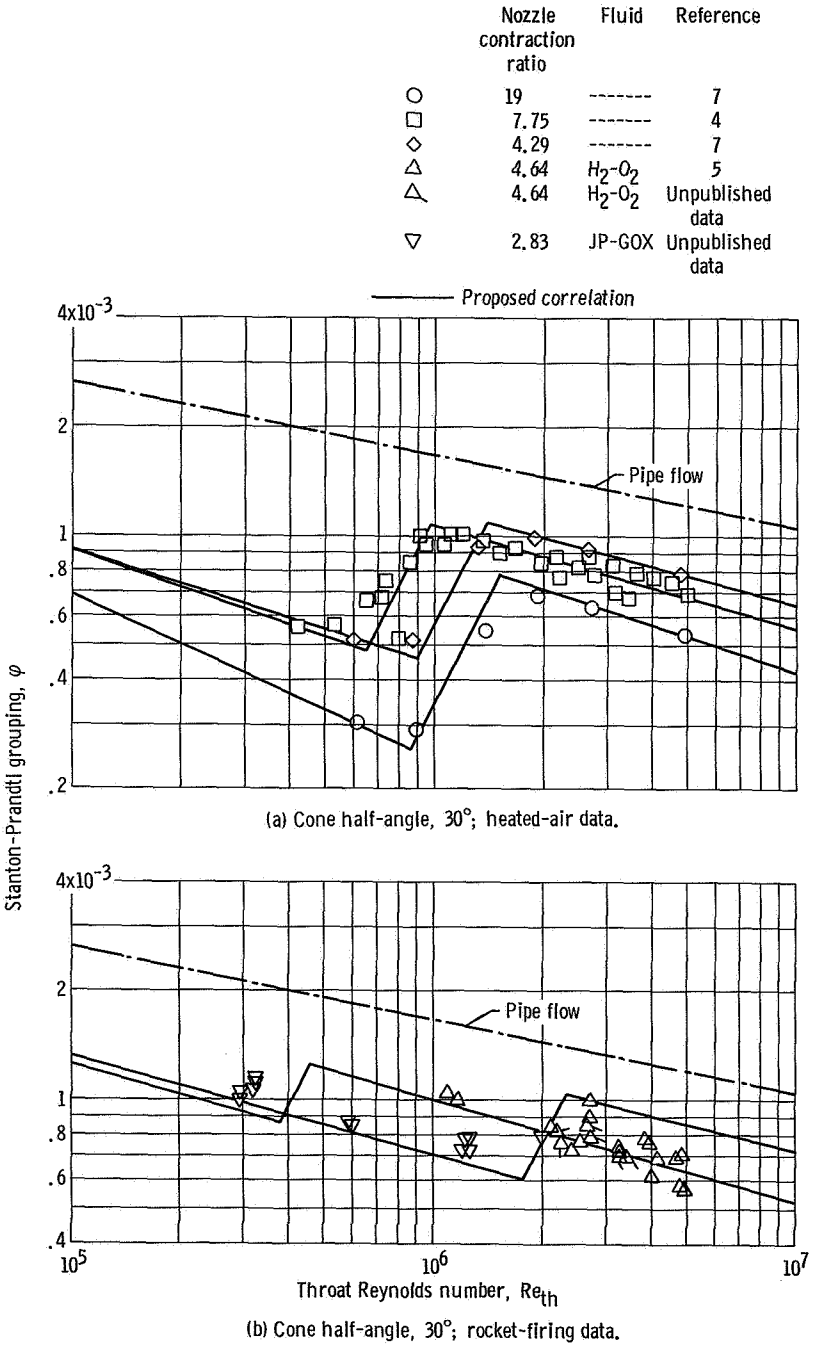

(a) Cone half-angle, 30°; heated-air data.

(b) Cone half-angle, 30°; rocket-firing data.

Figure 5. - Comparison of experimental data at nozzle throat station with pipe flow prediction and proposed correlation.

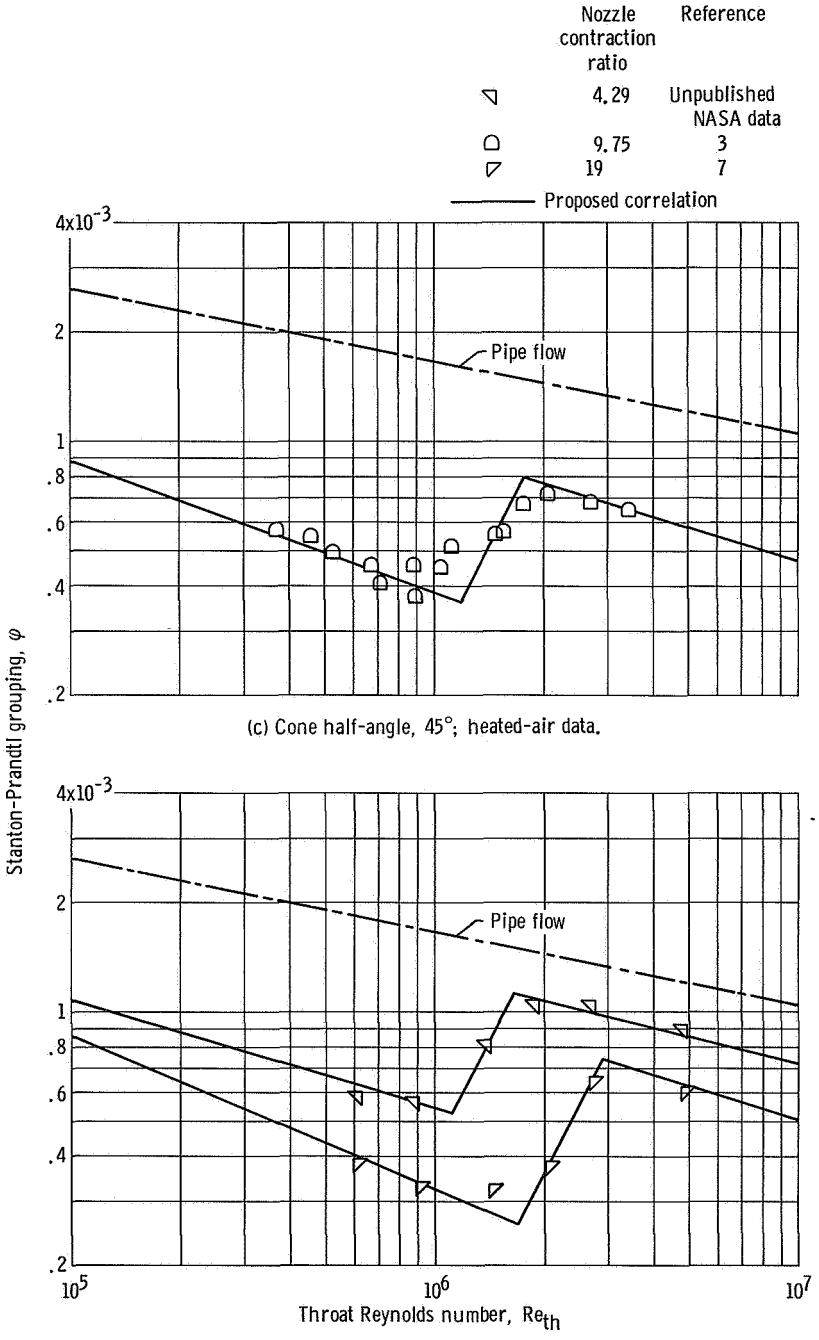

(c) Cone half-angle, 45°; heated-air data.

(d) Cone half-angle, 60°; heated-air data.

Figure 5. - Concluded.

Nozzle Contraction Section

The local heat transfer along the nozzle from the inlet to the throat, for convenience, is referenced to the throat heat transfer at the local Re value. In a strict sense, the location of the sonic point just upstream of the geometric throat should be used as a reference for choked flow. However, the ease in using the heat-transfer value at the geometric throat far outweighs the small error in heat transfer introduced for the axial region bounded by sonic point and the geometric throat.

As was the case for the throat region, the local heat-transfer values exhibit low Re and high Re characteristics as a function of local Re values. Correlation of heat transfer for these regions is given by the following equations, in which all φ values, unless specifically noted as in the case of the transition region, are based on the local Reynolds number.

Low Reynolds number region:

$$\varphi_L = \varphi_{th,L} + \left(\varphi_{pf} - \varphi_{th,L}\right)\left[\left(\frac{\frac{A}{A_{th}} - 1}{\frac{A_i}{A_{th}} - 1}\right)^{\sqrt{\sin\theta_c}} \left(\frac{1}{1 - \sin\theta_i} - \frac{\sin\theta_i}{\sin\theta_c}\right)^{0.115\sqrt{A_i/A_{th}}}\right] \tag{16}$$

Downstream of the point of tangency formed by the inlet curvature, r_{ci}, and the conical nozzle wall (or with r_c if a cone is not used in the contraction section) or for a sharp-cornered nozzle inlet as used in the NASA heated air nozzles, equation (16) reduces to

$$\varphi_L = \varphi_{th,L} + \left(\varphi_{pf} - \varphi_{th,L}\right)\left[\left(\frac{\frac{A}{A_{th}} - 1}{\frac{A_i}{A_{th}} - 1}\right)^{\sqrt{\sin\theta_c}} \left(\frac{\sin\theta_c}{1 - \sin\theta_c}\right)^{0.115\sqrt{A_i/A_{th}}}\right] \tag{17}$$

High Reynolds number region:

$$\varphi_T = \varphi_{th,T} + \left(\varphi_{pf} - \varphi_{th,T}\right)\left[0.2\left(\frac{A_{TAN}}{A_{th}}\right)\left(\frac{r_c}{r_{th}}\right)^{0.33}\left(\frac{A_i}{A_{th}}\right)^{0.5}\left(\frac{\frac{A}{A_{th}} - 1}{\frac{A_i}{A_{th}} - 1}\right)^{0.23\sqrt{(A_i/A_{th})\sin\theta_c}}\right] \tag{18}$$

The absolute values of the product of the terms within the brackets in equation (18) are valid in the limits of 0 to 1.0.

Transition region: - In the transition region between the low Re and high Re regions the local heat transfer is calculated by the following relation:

$$\varphi_{Tran} = \left(\varphi_L\right)_{Re'_{TL}}\left(\frac{Re}{Re'_{TL}}\right) \tag{19}$$

where the value of the Reynolds number at which the transition region begins is evaluated from the local low Re curve as follows:

$$Re'_{TL} = \left(Re_{TL}\right)\left[1 + \frac{\left(\frac{A}{A_{th}} - 1\right)}{\left(\frac{A_i - A}{A_{th}}\right)}\right]^{\left(A_{th}/A\right)^{0.033\left(A_i/A_{th}\right)}} \tag{20}$$

The transition region terminates when φ_{Tran} equals φ_T at the same value of Re.

It should be noted that in the contraction section of a nozzle the value of φ for all stations upstream of the sonic point is a direct function of the local Reynolds number to the first order. This is in contrast to the throat station and to the stations in the supersonic region of the nozzle for which a square law variation with Reynolds number occurs.

Comparisons of typical local heat-transfer data with calculated values for the contraction sections of several nozzles are shown in figure 6. The major discrepancies between calculated and experimental values occur near the nozzle entrance. This is to be expected because of local corner flow separation effects and flow distortions due to the local curvature of the wall. These effects die out quickly once the flow has turned com-

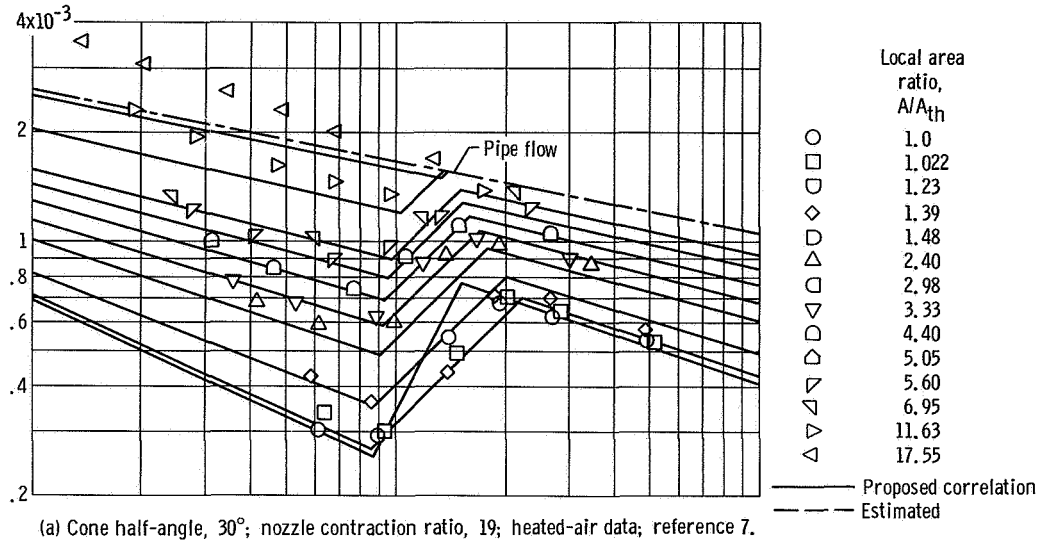

(a) Cone half-angle, 30°; nozzle contraction ratio, 19; heated-air data; reference 7.

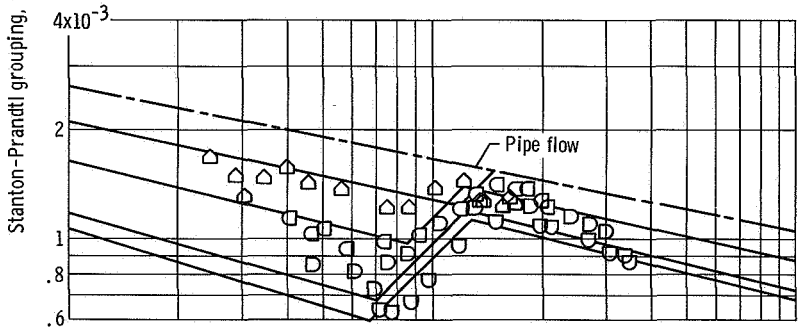

(b) Cone half-angle, 30°; nozzle contraction ratio, 7.75; heated-air data (air temperature, 1500° F (1089 K)); reference 4.

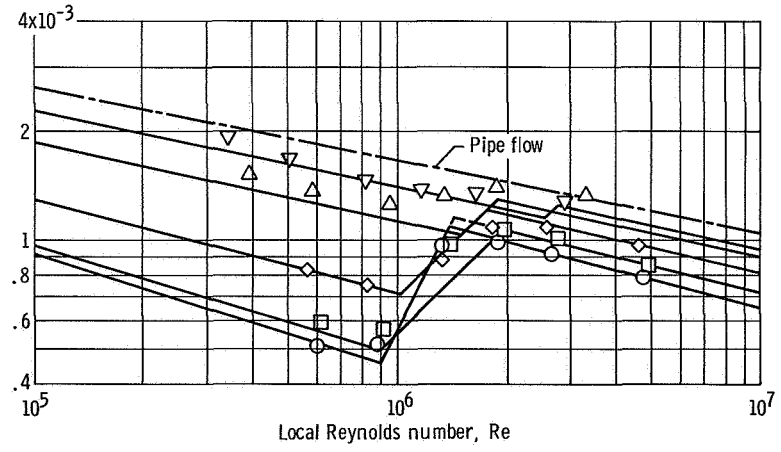

(c) Cone half-angle, 30°; nozzle contraction ratio, 4.29; heated-air data; unpublished NASA data.

Figure 6. - Comparison of experimental data in nozzle contraction section with pipe flow prediction and proposed correlation

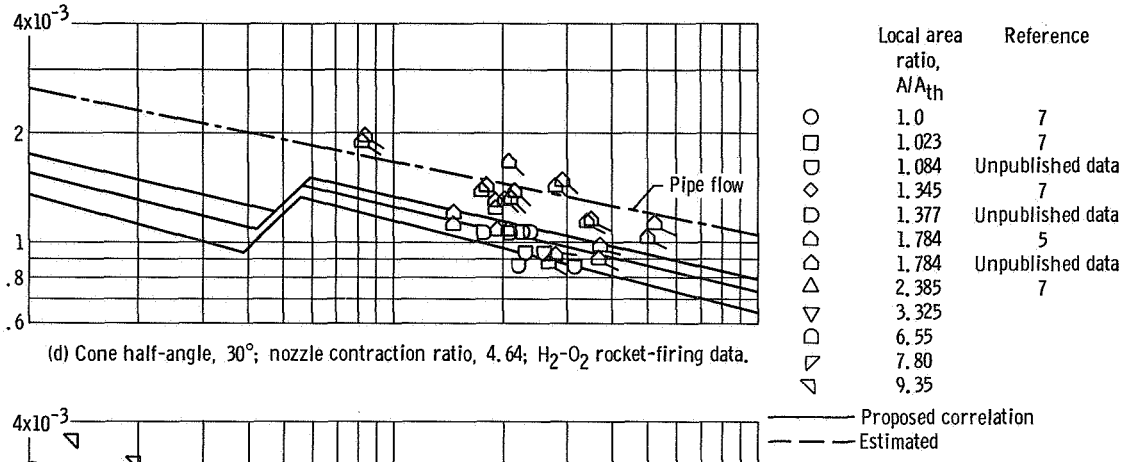

(d) Cone half-angle, 30°; nozzle contraction ratio, 4.64; H_2-O_2 rocket-firing data.

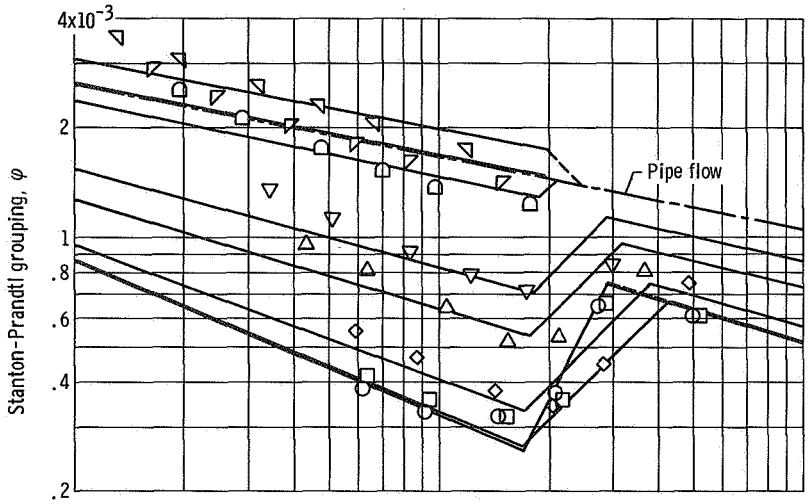

(e) Cone half-angle, 60°; nozzle contraction ratio, 19; heated-air data; reference 7.

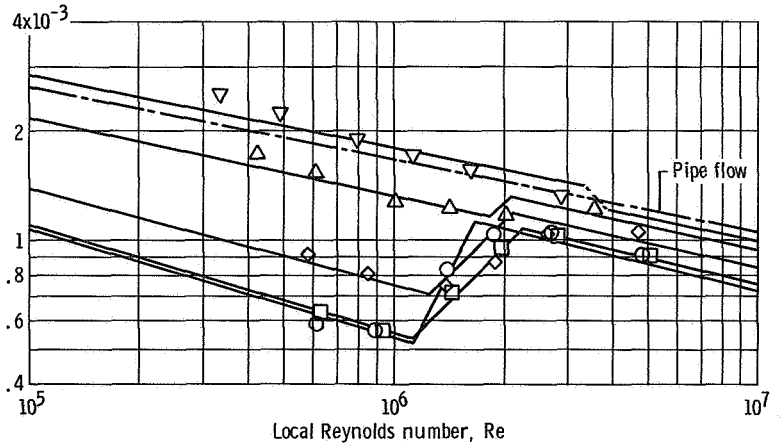

(f) Cone half-angle, 60°; nozzle contraction ratio, 4.29; heated-air data; unpublished NASA data.

Figure 6. - Concluded.

pletely and follows the conical walls of the nozzle. It is also apparent that for the nozzles in figures 6(c) and (e) and possibly in figure 6(f), the station designated by $(A/A_{th}) = 1.023$ is a sonic point station or just downstream of it as evidenced by the fact that the transition region slope follows the square law relation with Re rather than a first-order law.

Nozzle Effuser Section

The local heat transfer in the divergent or effuser section also was related to that at the throat station and all φ values (including throat) in the following equations are based on local Re values unless otherwise noted.

Low Reynolds number region: - Insufficient data was available to permit the development of correlating equations. The data that were available, however, indicated that a low Re region similar to that in the contraction cone can exist in the supersonic regions of the effuser.

High Reynolds number region:

$$\varphi_T = \varphi_{th,T} + \left(\varphi_{pf} - \varphi_{th,T}\right)\left[6.0\left(\frac{r_c}{r_{th}}\right)\left(\frac{x}{D}\right)\left(\sin\theta_c\right)\left(\frac{A_{th}}{A_i}\right)^{0.8}\right] \tag{21}$$

The absolute values of the product of the terms within the brackets in equation (21) are valid in the limits of 0 to 1.0.

Transition region:

$$\varphi_{Tran} = \left(\varphi_T\right)_{Re'_{TT}}\left(\frac{Re}{Re'_{TT}}\right)^{2.0} \tag{22}$$

where

$$Re'_{TT} = Re_{TT}\left[1 - \left(\frac{x}{D}\right)\left(\frac{A_{th}}{A}\right)^{0.5\left(\sin\theta_c\right)^{1.33}}\right] \tag{23}$$

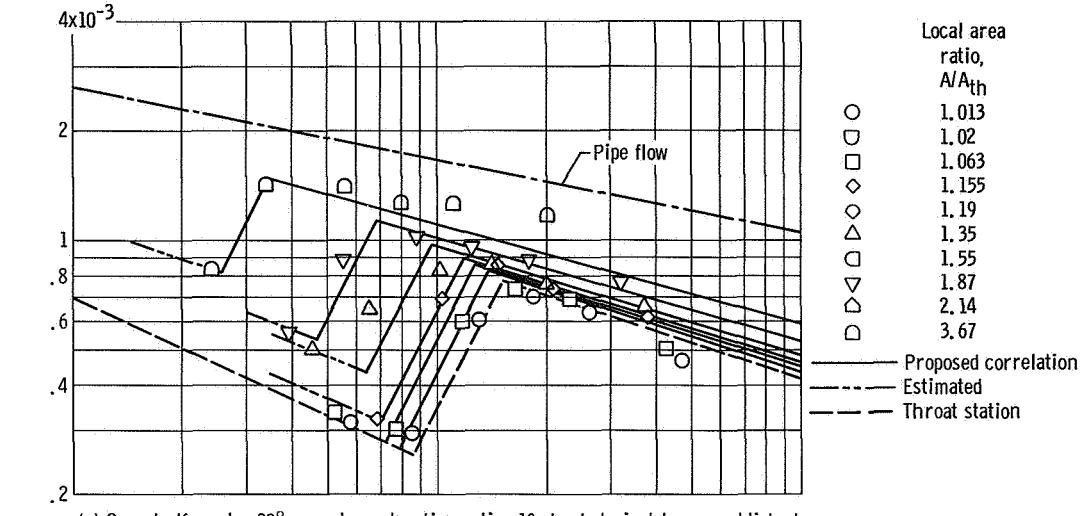

(a) Cone half-angle, 30°; nozzle contraction ratio, 19; heated-air data; unpublished NASA data.

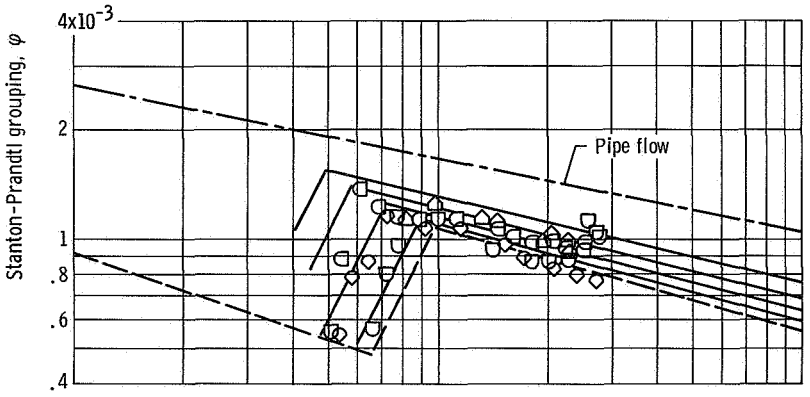

(b) Cone half-angle, 30°; nozzle contraction ratio, 7.75; heated-air data (air temperature, 1500° F (1089 K)); reference 4.

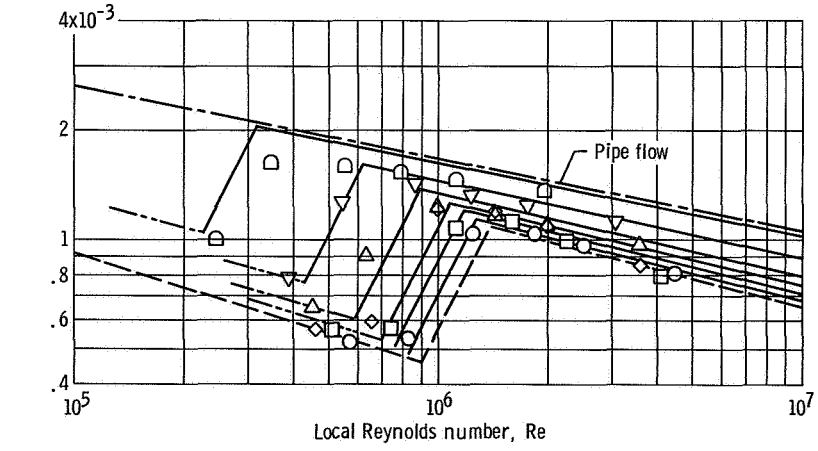

(c) Cone half-angle, 30°: nozzle contraction ratio, 4.29; heated-air data; unpublished NASA data.

Figure 7. - Comparison of experimental data in nozzle divergent section with pipe flow prediction and proposed correlation.

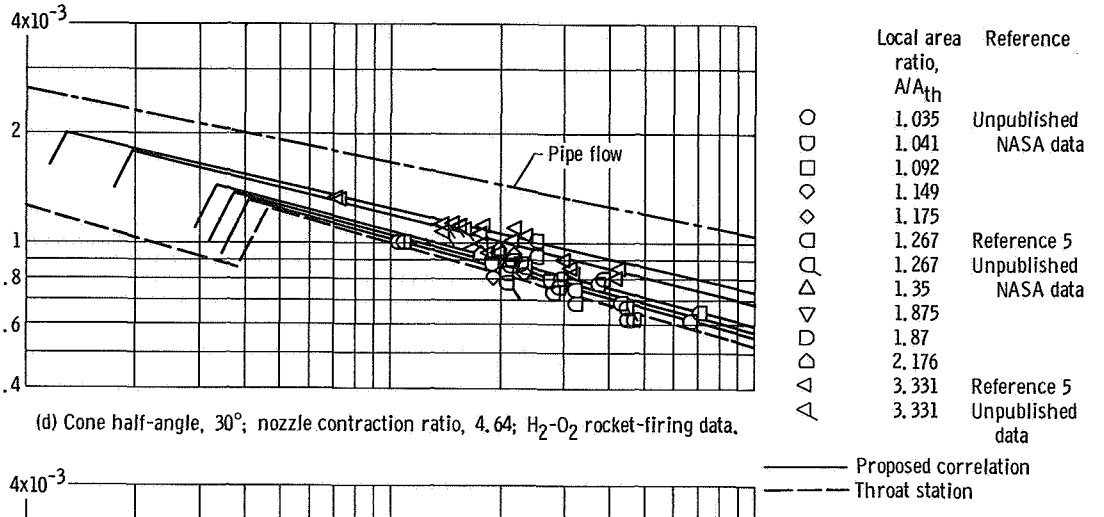

(d) Cone half-angle, 30°; nozzle contraction ratio, 4.64; H_2-O_2 rocket-firing data.

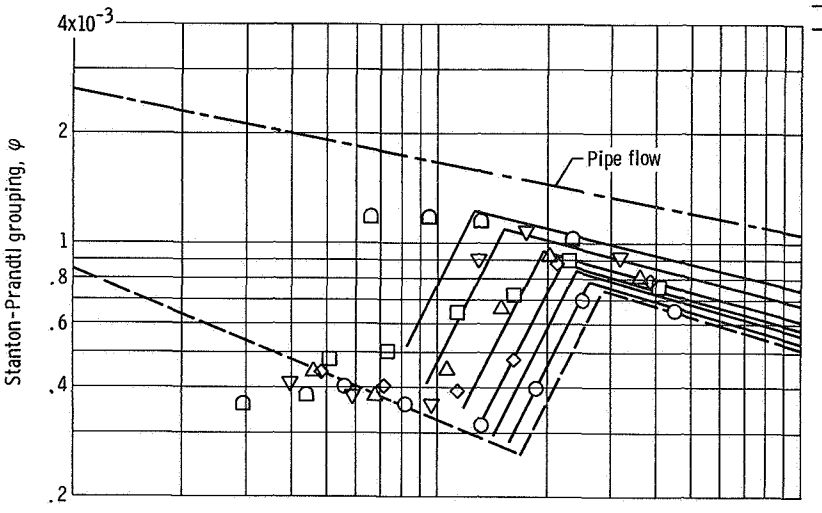

(e) Cone half-angle, 60°; nozzle contraction ratio, 19; heated-air data; unpublished NASA data.

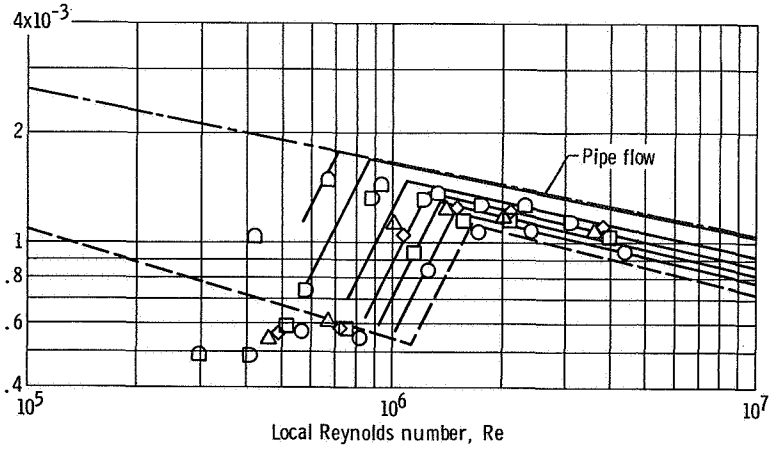

(f) Cone half-angle, 60°; nozzle contraction ratio, 4.29; heated-air data; unpublished NASA data.

Figure 7. - Concluded.

The lower limit for φ_{Tran} cannot be established due to insufficient data for correlation. However, for a fully flowing effuser, the φ_{Tran} values should not fall below the values calculated for $\varphi_{th,L}$.

The need for including the contraction cone half-angle, θ_c, in equations (21) and (23) for the diffuser is interpreted, in a gross sense, as representing an influence on the contraction section on the boundary layer entering the diffuser section.

Analysis of the data in the effusers was limited to a cone half-angle, θ_e, of 15^o; consequently it was not possible to include the effect of this variable in the correlation equations. Equations (21) and (23) both include terms of local area ratio and distance from the nozzle throat. These two parameters were deliberately chosen so that convergent nozzles with as well as without effusers could be analyzed. A cursory check of the heat-transfer data for the nozzle configuration of reference 6 (no effuser) indicates that reasonable local heat-transfer values would be predicted by equation (21).

Comparisons of typical local heat-transfer data with calculated values and pipe-flow predictions are shown in figure 7 for several nozzle effuser sections. Even though the flow through the effusers was, for the most part, supersonic and full, local separation effects at the point of tangency between the throat curvature, r_c, and the conical effusers used for all nozzles (cone half-angle, 15^o) could be detected in the data (see also ref. 3). Furthermore, at the lowest system pressures used in the experimental studies, significant flow separation occurred near the effuser exit stations. Data that showed obvious separation characteristics were excluded from comparison with the empirical correlation equations; however, marginal data were included and are easily recognized in the data plots.

For the case of subsonic flow through an effuser, it is believed that the slope of the transition curve is 1.0, however, data to verify this conjecture were not available to the author.

CONCLUDING REMARKS

The empirical correlating equations proposed herein have all the obvious shortcomings of such correlations; namely, the direct use is necessarily limited to the configurations used in the development of the equations. However, the large range of variables included in these configurations permits, in the author's opinion, the extrapolating of the correlation over a reasonable extent of the parameters involved.

Some of the rocket nozzle heat-transfer work prior to 1965, while exhibiting trends similar to the data used herein, yields much higher heat-transfer values. Indeed, the values at the throat station in the high Reynolds number (turbulent-like) region exceed pipe flow values. In the author's opinion these data are similar to the NASA heated-air data (refs. 8 and 9) which show the combined effects of configuration geometry and of a

wall-temperature step change near the nozzle entrance on nozzle heat transfer. It is suggested that the effects of such a temperature step change could be approximated by using a method of superposition type of analysis. By this is meant the addition of the heat-transfer increment caused by a temperature step change for pipe flow to the nozzle heat transfer calculated by the correlation developed herein. Consideration of such a technique is beyond the scope of the present study due to the limited information available to establish suitable and necessary parameters.

In addition, Stanton-Prandtl grouping values higher than those predicted by the proposed correlation also can be expected when a chemical rocket engine injector or a nuclear rocket core causes inadvertent "jet" impingement on the contraction core (particularly near the throat) or when the approach section (combustion chamber or transition section between a core and the nozzle) length-to-diameter ratio is very small. The latter problem is an entrance effect similar to that commonly experienced with heated tube studies. Both of these problems are, unfortunately, beyond the scope of the present correlation.

In the final analysis, the present empirical method should be considered only as a stop-gap measure. Further research is necessary to predict the correct development of the boundary layer in a nozzle and the accompanying temperature gradients when the nozzle walls are cooled. Only by such studies can a satisfactory nozzle heat-transfer analysis be achieved.

Lewis Research Center,
National Aeronautics and Space Administration,
Cleveland, Ohio, December 5, 1968,
122-29-07-06-22.

APPENDIX - SYMBOLS

A	local area, ft^2; m^2
A_i	nozzle inlet area, ft^2; m^2
A_{TAN}	area at wall inflection (tangency) point with throat radius of curvature, ft^2; m^2
A_{th}	throat area, ft^2; m^2
a, a_L, a_T	exponents in correlation equations
C, C_L, C_T	constants in correlation equations
D	local diameter, ft; m
D_{th}	throat diameter, ft; m
L	surface distance measured along wall from nozzle inlet to throat, ft; m
Nu	Nusselt number
Pr	Prandtl number
Re	local Reynolds number
Re_{th}	throat Reynolds number
r_c	wall radius of curvature at throat, ft; m
r_{ci}	wall radius of curvature at inlet, ft; m
r_i	nozzle inlet radius, ft; m
r_{th}	throat radius, ft; m
St	Stanton number
x	distance along wall measured from throat downstream toward nozzle exit (effuser section), ft; m
θ_c	cone half-angle in contraction section, deg
θ_e	cone half-angle in effuser section, deg
θ_i	local wall half-angle near nozzle inlet, $(\theta_i < \theta_c)$, deg
φ	Stanton-Prandtl grouping, $\varphi = StPr^{0.7}$

Subscripts:

L	low Re
pf	pipe flow
T	high Re
TL	transition from low Re curve
TT	transition from high Re curve
th	throat
Tran	transition

Superscript:

	local value in transition region

REFERENCES

1. Bartz, D. R.: Turbulent Boundary-Layer Heat Transfer from Rapidly Accelerating Flow of Rocket Combustion Gases and of Heated Air. Advances in Heat Transfer. Vol. 2, J. P. Hartnett and T. F. Irvine, Jr., eds., Academic Press, Inc., 1965, pp. 1-108.

2. Ellicott, David G.; Bartz, Donald R.; and Silver, Sidney S.: Calculation of Turbulent Boundary-Layer Growth and Heat Transfer in Axi-Symmetric Nozzles. Rep. TR 32-387, Jet Propulsion Lab., California Inst. Tech., Feb. 15, 1963.

3. Back, L. H.; Massier, P. F.; and Cuffel, R. F.: Flow Phenomena and Convective Heat Transfer in a Conical Supersonic Nozzle. TR 32-1152, Jet Propulsion Laboratory, 1967 (Contract NAS7-100, NASA).

4. Back, L. H.; Massier, P. F.; and Gier, H. L.: Convective Heat Transfer in a Convergent-Divergent Nozzle. Rep. TR-32-415, rev. 1, Jet Propulsion Lab., California Inst. Tech. (NASA CR-57326), Feb. 15, 1965.

5. Schacht, Ralph L.; Quentmeyer, Richard J.; and Jones, William L.: Experimental Investigation of Hot-Gas Side Heat-Transfer Rates for a Hydrogen-Oxygen Rocket. NASA TN D-2832, 1965.

6. Moretti, P. M.; and Kays, W. M.: Heat Transfer to a Turbulent Boundary Layer with Varying Free-Stream Velocity and Varying Surface Temperature - An Experimental Study. Int. J. Heat Mass Transfer, vol. 8, no. 9, Sept. 1965, pp. 1187-1202.

7. Boldman, Donald R.; Schmidt, James F.; and Gallagher, Anne K.: Laminarization of a Turbulent Boundary Layer as Observed from Heat-Transfer and Boundary-Layer Measurements in Conical Nozzles. NASA TN D-4788, 1968.

8. Boldman, D. R.; Schmidt, J. F.; and Ehlers, R. C.: Effect of Uncooled Inlet Length and Nozzle Convergence Angle on the Turbulent Boundary Layer and Heat-Transfer in Conical Nozzles Operating with Air. J. Heat Transfer, vol. 89, no. 4, Nov. 1967, pp. 341-350.

9. Boldman, Donald R.; Neumann, Harvey E.; and Schmidt, James F.: Heat Transfer in 30° and 60° Half-Angle of Convergence Nozzles with Various Diameter Uncooled Pipe Inlets. NASA TN D-4177, 1967.

NASA-Langley, 1969 —— 33 E-4770

NATIONAL AERONAUTICS AND SPACE ADMINISTRATION
WASHINGTON, D.C. 20546
OFFICIAL BUSINESS

FIRST CLASS MAIL

POSTAGE AND FEES PAID
NATIONAL AERONAUTICS AND
SPACE ADMINISTRATION

POSTMASTER: If Undeliverable (Section 158
Postal Manual) Do Not Return

"The aeronautical and space activities of the United States shall be conducted so as to contribute . . . to the expansion of human knowledge of phenomena in the atmosphere and space. The Administration shall provide for the widest practicable and appropriate dissemination of information concerning its activities and the results thereof."

—NATIONAL AERONAUTICS AND SPACE ACT OF 1958

NASA SCIENTIFIC AND TECHNICAL PUBLICATIONS

TECHNICAL REPORTS: Scientific and technical information considered important, complete, and a lasting contribution to existing knowledge.

TECHNICAL NOTES: Information less broad in scope but nevertheless of importance as a contribution to existing knowledge.

TECHNICAL MEMORANDUMS: Information receiving limited distribution because of preliminary data, security classification, or other reasons.

CONTRACTOR REPORTS: Scientific and technical information generated under a NASA contract or grant and considered an important contribution to existing knowledge.

TECHNICAL TRANSLATIONS: Information published in a foreign language considered to merit NASA distribution in English.

SPECIAL PUBLICATIONS: Information derived from or of value to NASA activities. Publications include conference proceedings, monographs, data compilations, handbooks, sourcebooks, and special bibliographies.

TECHNOLOGY UTILIZATION PUBLICATIONS: Information on technology used by NASA that may be of particular interest in commercial and other non-aerospace applications. Publications include Tech Briefs, Technology Utilization Reports and Notes, and Technology Surveys.

Details on the availability of these publications may be obtained from:

SCIENTIFIC AND TECHNICAL INFORMATION DIVISION

NATIONAL AERONAUTICS AND SPACE ADMINISTRATION

Washington, D.C. 20546